Materials Transactions, Vol. 63, No. 7 (2022) pp. 1072 to 1079

Antibacterial Properties and Biocompatibility of Hydroxyapatite Coating Doped with Various Cu Contents on Titanium

Qiang Li[1,2,*], Shihong Song[1], Junjie Li[3], Jinshuai Yang[1], Ran Zhang[1], Mitsuo Niinomi[1,4,5,6,7,*] and Takayoshi Nakano[5]

[1]*School of Mechanical Engineering, University of Shanghai for Science and Technology, Shanghai 200093, P. R. China*
[2]*Shanghai Engineering Research Center of High-Performance Medical Device Materials, Shanghai 200093, P. R. China*
[3]*CAS Key Laboratory of Functional Materials and Devices for Special Environments, Xinjiang Technical Institute of Physics & Chemistry, CAS; Xinjiang Key Laboratory of Electronic Information Materials and Devices, 40-1 South Beijing road, Urumqi 830011, P. R. China*
[4]*Institute for Materials Research, Tohoku University, Sendai 980-5377, Japan*
[5]*Division of Materials and Manufacturing Science, Graduate School of Engineering, Osaka University, Suita 565-0871, Japan*
[6]*Department of Materials Science and Engineering, Graduate School of Science and Technology, Meijo University, Nagoya 468-8502, Japan*
[7]*Faculty of Chemistry, Materials and Bioengineering, Kansai University, Osaka 564-8680, Japan*

To explore the effect of copper content in a copper-doped hydroxyapatite coating (CuHAp) on its antibacterial activity and biocompatibility, a layer of CuHAp was deposited on the surface of pure Ti using an electrochemical deposition method. An orthogonal experiment was used to determine the Cu content in the coating by varying the concentration of Cu^{2+} in the electrolyte. The antibacterial properties and biocompatibility of the CuHAp coatings were also evaluated. The antibacterial effect increased with increasing Cu content in the sample. When the content of Cu in the coating was 1.57%, the deposited CuHAp coating exhibited excellent biocompatibility, and the number of living cells after culturing was significantly higher than that for the HAp coating. When the content of Cu increased to 6.85%, the coating exhibited cytotoxicity. Thus, the CuHAp sample with a Cu content of 1.57% exhibited good antibacterial and biocompatibility, and thus could be a suitable material for use in biomedical applications. [doi:10.2320/matertrans.MT-M2021245]

(Received December 14, 2021; Accepted April 19, 2022; Published June 3, 2022)

Keywords: *hydroxyapatite, copper, orthogonal experiment, antibacterial coating, biocompatibility*

1. Introduction

Ti and its alloys are widely used in biomedical fields because of their excellent mechanical properties and good biocompatibility.[1,2] However, as clinical implant materials, Ti and its alloys have some disadvantages, such as poor antibacterial and biological activity, poor chemical binding with surrounding tissues, and a tendency to induce inflammation.[3–5] Therefore, solving these disadvantages through surface modification is critical. To further enhance the bone integration abilities and antibacterial properties of implants, metal implants are usually coated with a layer of bone-inducing biomaterials such as calcium silicate, carbon nanotube (CNT)-reinforced chitosan-based ceramics,[6] and hydroxyapatite (HAp) bioceramics.

HAp is a hexagonal crystal system with the same chemical composition as bone.[7] It is widely used as a coating material for metal implants because of its excellent bone conductivity and biocompatibility and because it does not induce inflammation in organisms.[8,9] HAp can provide biomedical metal substrates with good mechanical and biological properties.[10] Jose *et al.* confirmed that HAp coatings on the surfaces of implants can promote bone formation.[11] However, a single HAp coating lacks antibacterial properties, which affects its long-term stability and leads to implant failure,[12] greatly limiting its clinical application. Therefore, improving the antibacterial properties of coatings by adding metal elements has been widely studied.

The antibacterial properties of HAp can be improved by various chemical modifications, such as cation and anion doping.[13,14] Some metal ions have strong antibacterial capabilities, but they may also lead to poor biocompatibility. Ag^{+} and Cu^{2+} have been proven to have better antibacterial activity than other metal ions.[15,16] However, the long-term presence of Ag in the human body can lead to major health problems.[17] In contrast, Cu, in addition to its antibacterial properties, is an essential trace element for the human body.[18,19] Recently, Cu has been used to improve the antibacterial properties of HAp coatings, and many studies have shown that changes in the Cu content significantly affect the antibacterial properties of the coatings. For example, Hang *et al.* prepared Ti–Cu–O nanotubes (NTs) with different Cu contents using pulsed DC magnetron sputtering.[20] It was found that the cytocompatibility of the NTs was closely related to the Cu content. When the Cu content was 1%, the NTs exhibited more normal antibacterial activity and cytocompatibility. Stranak *et al.* prepared Ti–Cu thin films on the surface of a Ti alloy by magnetron sputtering, which showed good antibacterial properties and no cytotoxicity to osteoblasts.[21] Wu prepared TiO_2 antibacterial coatings with different Cu contents on pre-sputtered CuTi films using a micro-arc oxidation technology. It was found that the antibacterial activity increased with increasing Cu content.[22] In addition, it has been proven that the deposition time and electrolyte temperature have significant effects on the surface morphology of the coating.[23,24] However, in addition to ensuring the antibacterial properties of the coating, ensuring the biocompatibility of the coating is also necessary. Therefore, in this study, we explored the effects of Cu

*Corresponding authors, E-mail: jxli@tju.edu.cn & liqiang@usst.edu.cn; mitsuo.niinomi.b6@tohoku.ac.jp

content on the antibacterial performance and cell compatibility of CuHAp coatings that were prepared on the surface of pure Ti via electrochemical deposition. The effects of Cu^{2+} concentration in the electrolyte as well as the deposition time and temperature on the copper content of the coating were studied through an orthogonal experiment. The coatings were characterized using an X-ray diffraction (XRD), a scanning electron microscopy (SEM), an X-ray photoelectron spectroscopy (XPS), and an energy dispersive spectroscopy (EDS). The antibacterial effects of the CuHAp coatings with different Cu contents were evaluated using Escherichia coli (*E. coli*) and Staphylococcus aureus (*S. aureus*). A methyl thiazolyl tetrazolium (MTT) assay was used to detect the activity of MC3T3-E1 cells inoculated on a HAp coating and CuHAp coatings with different Cu contents.

2. Experimental Method

2.1 Orthogonal experiment

Commercial pure Ti sheets [purity of 99.5%, ZhongNuo Advanced Material (Beijing) Technology Co., Ltd.] with dimensions of 10 mm × 10 mm were used as the substrates. The pure Ti sheets were polished with sandpaper and ultrasonically cleaned. They were then pickled with a mixed acid of HF and HNO_3 for 30 s. After ultrasonic cleaning in deionized water, the sheets were dried in an oven at 80°C for 1 h. A double-electrode system was adopted, in which the anode and cathode were platinum and the pretreated pure Ti sheets, respectively. The distance between the two electrodes was 2 cm, and the deposition voltage was 3 V. Analytical grade $CaCl_2{\cdot}2H_2O$, $NH_4H_2PO_4$, and $CuCl_2{\cdot}2H_2O$ were used as the sources of Ca, P, and Cu, respectively. A NaCl solution (0.1 mol/L) was added to increase the conductivity of the electrolyte. The beaker containing the electrolyte was placed in a constant-temperature water bath for thermal insulation to ensure a stable temperature during the deposition process.

The copper content of the coating was controlled by changing three electrochemical deposition conditions: Cu^{2+} concentration in the electrolyte, deposition time, and deposition temperature. Table 1 lists the factor levels used in the orthogonal experiment. The Cu^{2+} content in the electrolyte was controlled by adjusting the n(Cu)/n(Ca) ratio with a fixed n(Cu + Ca)/n(P) ratio of 1.68. Table 2 shows the compositions of the electrolytes with different Cu^{2+} concentrations corresponding to Table 1.

Table 1 Factor levels of orthogonal experiment.

Level	Factor		
	Cu^{2+} concentration in electrolyte (A) / mmol / L	Deposition time (B) / min	Deposition temperature(C) / °C
1	4.200	30	55
2	2.100	22.5	45
3	1.050	15	35
4	0.525	7.5	25

Table 2 Compositions of the electrolytes with different n(Cu)/n(Ca) ratios.

Group	$CuCl_2$ / mmol/L	$CaCl_2$ / mmol/L	$NH_4H_2PO_4$ / mol/L	n(Cu)/n(Ca)
(a)	0.525	41.475	0.025	1/79
(b)	1.05	40.95	0.025	1/39
(c)	2.10	39.9	0.025	1/19
(d)	4.20	37.8	0.025	1/9

Table 3 Results of orthogonal experimental scheme.

Number	Factors			Results
	Cu^{2+} concentration in electrolyte (A)/ mmol/L	Deposition time (B)/ min	Deposition temperature (C) / °C	Copper content (mass.%)
1	4.2	30	55	25.37
2	4.2	22.5	45	15.21
3	4.2	15	35	9.82
4	4.2	7.5	25	3.56
5	2.1	30	45	8.43
6	2.1	22.5	55	12.33
7	2.1	15	25	3.68
8	2.1	7.5	35	3.66
9	1.05	30	35	3.99
10	1.05	22.5	25	4.61
11	1.05	15	55	4.92
12	1.05	7.5	45	1.57
13	0.525	30	25	3.57
14	0.525	22.5	35	2.77
15	0.525	15	45	3.98
16	0.525	7.5	55	2.22

Based on the Cu^{2+} concentrations, deposition times, and deposition temperatures, an $L_{16}(4^3)$ orthogonal experiment table (Table 3) was constructed with three factors and four levels, with the Cu content in the prepared coating taken as the evaluation index. CuHAp coatings 1–16 were prepared by electrochemical deposition following the abovementioned steps according to the three fixed factors (Cu^{2+} concentration, deposition time, and deposition temperature) in Table 3. The influence of the order of three electrochemical deposition conditions on the Cu content of the coatings was determined.

2.2 Preparation of CuHAp in the electrolytes with different Cu^{2+} concentrations

According to the results of the orthogonal experiment (see

Section 3.1), the CuHAp coatings were prepared in electrolytes with different Cu^{2+} concentrations, as listed in Table 2. For comparison, a HAp coating without Cu was prepared in an electrolyte containing 0.042 mol/L $CaCl_2$ and 0.025 mol/L $NH_4H_2PO_4$. The deposition voltage, time, and temperature were 3 V, 7.5 min, and 45°C, respectively. Also, 0.1 mol/L NaCl was added to increase the conductivity of the electrolyte.

2.3 Surface characterization

The surface morphology of the coating was observed and analyzed using an SEM (FEI Quanta 450FEG) with an accelerating voltage of 30 kV, and the elements in the coating were analyzed using an EDS. The phase compositions of the coatings were tested using an XRD (Bruker D8 Advance, Germany) with Cu Kα radiation at a voltage of 40 kV, a current of 40 mA, and a scanning speed of 6°/min. The chemical state of Cu in the coating was analyzed by XPS (AIXS Ultra DLD) with a monochromatic Al Kα ($h\nu =$ 1486.6 eV) X-ray radiation source.

2.4 Antibacterial test

Gram-negative *E. coli* (ATCC25922) and gram-positive *S. aureus* (ATCC29213) were used as test strains for analysis. The liquid medium was prepared by mixing 1 g of peptone, 0.5 g of yeast powder, and 1 g of NaCl in 100 mL of distilled water. The solid medium was prepared by mixing 1 g of peptone, 0.5 g of yeast powder, 1 g of NaCl, and 1.5 g of agar powder in 100 mL of distilled water. To prepare the bacterial suspension, single colonies of *E. coli* and *S. aureus* were selected from the solid medium, and each colony was placed into a tube containing 3 mL of liquid medium. A tube containing 3 mL of liquid medium was used as the blank control. The three tubes were placed in a constant-temperature oscillator at 37°C at a speed of 200 rpm for 15 h.

The samples coated with HAp and CuHAp were subjected to an antibacterial test. All samples were sterilized under a high temperature of 121°C and high pressure for 15 min and then put into a 24-well plate. The bacterial solution was first diluted to 10^6 CFU/mL in liquid medium, and then 0.2 mL of the diluted bacterial solution was added to each sample surface. To prevent volatilization of the liquid bacterial water, an appropriate amount of sterile normal saline was placed into each empty hole.

The 24-well plate was then placed in a constant-temperature incubator at 37°C and co-cultured for 24 h. After that, the co-culture solution was diluted 10^6 times with sterile phosphate-buffered saline solution (PBS; Procell Life Science & Technology Co., Ltd.), and then 100 µL of diluen was obtained using a pipette gun and evenly coated on the solid medium in a Petri dish with diameter of 90 mm. After incubation at 37°C in a constant-temperature incubator for 24 h, the colony number of each Petri dish was recorded. The antibacterial rate (η) of the coatings was calculated using the following formula:[25]

$$\eta = \frac{A - B}{A} \times 100\%$$

where A and B are the numbers of the blank control and the test sample colonies, respectively.

2.5 Cytocompatibility test

The mouse pre-osteoblast line MC3T3-E1 (iCell Bioscience Inc., Shanghai, China) was used to evaluate the cytotoxicity of the alloys. The culture medium was α-MEM (Corning Inc.) supplemented with 10% fetal bovine serum (FBS; Biological Industries). Pure Ti and the samples coated with HAp and CuHAp were selected to study their cytocompatibility. The samples were sterilized at high temperature and high pressure. Because the samples were all solid flakes, extraction was carried out at 37°C for 24 h with the surface area to extract a liquid volume ratio of 1.25 cm^2/mL following the ISO10993-12 standard. Each sample extract (100 µL) was placed into a 96-well plate separately, and three parallel wells were set up for each sample. The MC3T3-E1 cells were seeded into each well at 2×10^3 cells/well for 1-day culturing and at 1×10^3 cells/well for 4- and 7-day culturing. As a control, MC3T3-E1 cells were seeded directly into the bottom of the wells. The 96-well plates were placed in a humidified incubator at 37°C in a 5% CO_2 atmosphere for 1, 4, or 7 days. After culturing, each well was rinsed three times with PBS. The culture medium (100 µL) with 10% MTT was added to each well and incubated in a humidified incubator at 37°C with a 5% CO_2 atmosphere for an additional 4 h. The supernatant was aspirated, and 100 µL of dimethyl sulfoxide (DMSO) was added to each well, followed by gentle shaking for 10 min. The optical density (OD) was measured at 570 nm using a TECAN SPARK 10M enzyme-labeled instrument.

2.6 Statistical analysis

Statistical analyses were performed using one-way analysis of variance, followed by the Tukey–Kramer post-hoc test.

3. Results and Discussion

3.1 Orthogonal experimental analysis values

Table 3 presents the results of the orthogonal experimental scheme. The Cu content given in the table is based on the content of each element measured by EDS. To conduct a range analysis of the orthogonal experimental results, we took the average value of the Cu content measured at each level for each factor. For example, K_1 represents the average value of the four groups of copper content when the Cu^{2+} concentration was 4.2 mmol/L. Then, the minimum value was subtracted from the maximum average value of each factor to obtain the range of the three factors.[26] The greater the range value of a factor, the greater the influence of this factor on the results. The results of the range analysis are presented in Table 4. The range value of electrolyte concentration is 10.36, which is greater than those of 7.59 and 7.35 for the deposition time and temperature, respectively. Therefore, the order of the influencing factors in the deposition conditions is Cu^{2+} concentration (A) > deposition time (B) > deposition temperature (C). Because the Cu^{2+} concentration in the electrolyte had the greatest influence on the Cu content in the coating, the Cu content in the coating was controlled by changing the Cu^{2+} concentration in the electrolyte in subsequent experiments, with the deposition time and deposition temperature fixed at 7.5 min and 45°C, respectively.

Table 4 Analysis of Cu content range.

Calculated value	Factors		
	Cu^{2+} concentration in electrolyte(A) / mmol/L	Deposition time(B) / min	Deposition temperature (C) / °C
K1	13.49	10.34	11.21
K2	7.03	8.73	7.30
K3	3.77	5.60	5.06
K4	3.13	2.75	3.86
Range R_K	10.36	7.59	7.35

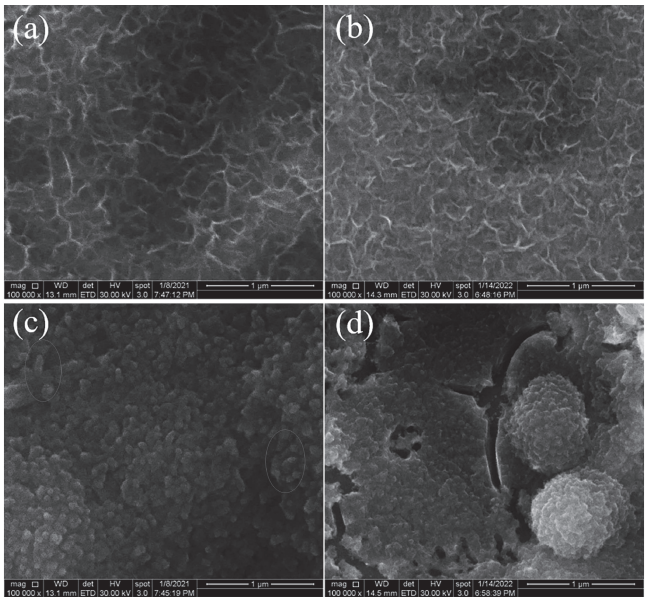

Fig. 1 Surface morphologies of the CuHAp coatings prepared in the electrolyte with different Cu^{2+} concentrations: (a) 0.525 mmol/L, (b) 1.05 mmol/L, (c) 2.1 mmol/L, and (d) 4.2 mmol/L.

3.2 Characterization of the coatings

Figure 1 shows the SEM images of the CuHAp coatings prepared at different electrolyte concentrations at a deposition time of 7.5 min and a deposition temperature of 45°C. When the Cu^{2+} concentration was 0.525 mmol/L, the CuHAp coating formed whisker-like crystals on the surface of the pure Ti sheet, as shown in Fig. 1(a). The Cu^{2+} concentration in the electrolyte was low, the reaction speed was slow, and the whisker-like crystals were thin and short. With increasing Cu^{2+} concentration, the Cu content in the coating gradually increased. When the Cu^{2+} concentration was 1.05 mmol/L, the CuHAp coating became dense, uniform, and honeycombed [Fig. 1(b)]. When the Cu^{2+} concentration was 2.1 mmol/L, rod-like crystals appeared in the CuHAp coating that were closely distributed on the surface of the pure Ti sheet, but they were not uniformly distributed [Fig. 1(c)]. When the Cu^{2+} concentration was 4.2 mmol/L, multiple cracks appeared in the CuHAp coating, which exhibited irregular blocks [Fig. 1(d)]. The porosity of the coating is an important factor. If the coating is too dense, it will not allow new tissue to grow inside its pores. If the coating is too porous, the aggressive media will penetrate this layer and the mechanical integrity of the implant will be compromised.[27] Thus, when the concentration of Cu^{2+} in the electrolyte was 1.05 mmol/L, the surface morphology of the coating was uniform and dense, and the pore size was suitable for cell attachment and growth. As shown in Fig. 2, with increasing Cu^{2+} concentration, the coating thickness increased from 281.7 nm to 892 nm. These results suggest that the increased Cu^{2+} concentration in the electrolyte promoted deposition of the coating.

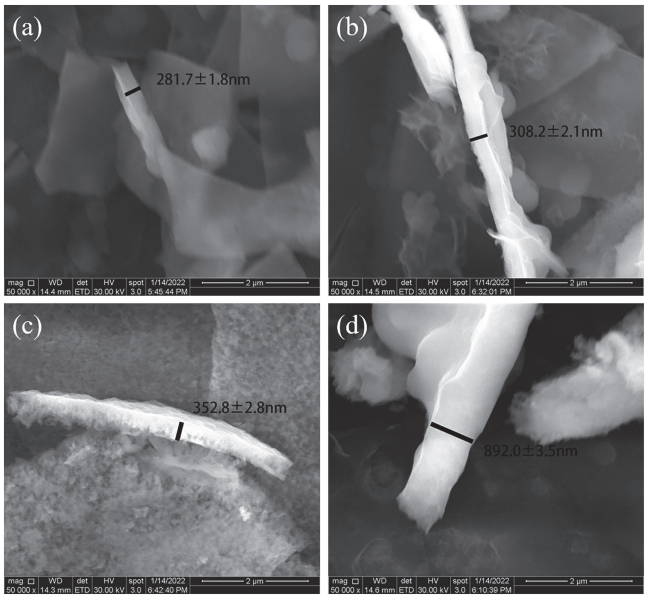

Fig. 2 SEM images for the thickness of the CuHAp coatings prepared in the electrolyte with different Cu^{2+} concentration: (a) 0.525 mmol/L, (b) 1.05 mmol/L, (c) 2.1 mmol/L, and (d) 4.2 mmol/L.

Figure 3 shows the XPS spectra of the main elements of the CuHAp coating under the following conditions: Cu^{2+} concentration of 1.05 mmol/L, deposition time of 7.5 min, and deposition temperature of 45°C. According to the high-resolution spectrum of Cu shown in Fig. 3(a), at binding energy (BE) values of 934.2 eV and 932.8 eV, the $Cu2p_{3/2}$ spectrum of the coating was composed of two components, Cu–OH and Cu–PO_4,[28] respectively. As shown in the high-resolution spectrum of P in Fig. 3(b), the peak at 133.0 eV corresponds to the BE value of P 2p, which corresponds to the BE value of the P–O bond in PO_4^{3-}, indicating that PO_4^{3-} was the main form of P in the CuHAp coating.[29] Figure 3(c) shows the high-resolution spectrum of Ca. The BE value of the $Ca2p_{3/2}$ peak is 347.0 eV and that of the $Ca2p_{1/2}$ peak is 350.5 eV, corresponding to the HAp compound. Figure 3(d) shows that the O 1s spectrum of all the investigated coatings consists of three components at binding energies of 529.9, 531.3, and 532.6 eV, which can be assigned to oxide species (O^{2-}), hydroxide and phosphate groups (OH^-, PO_4^{3-}), and adsorbed water (H_2O), respectively.[30] The trace oxide may have formed by the oxidation of the Ti sheet. Because the oxygen content was relatively low, it can be concluded that the coating did not contain CuO. The XPS results indicated that Cu replaced Ca in HAp.

Figure 4 shows the mapping of elements on the surface of the CuHAp coating formed when the concentration of

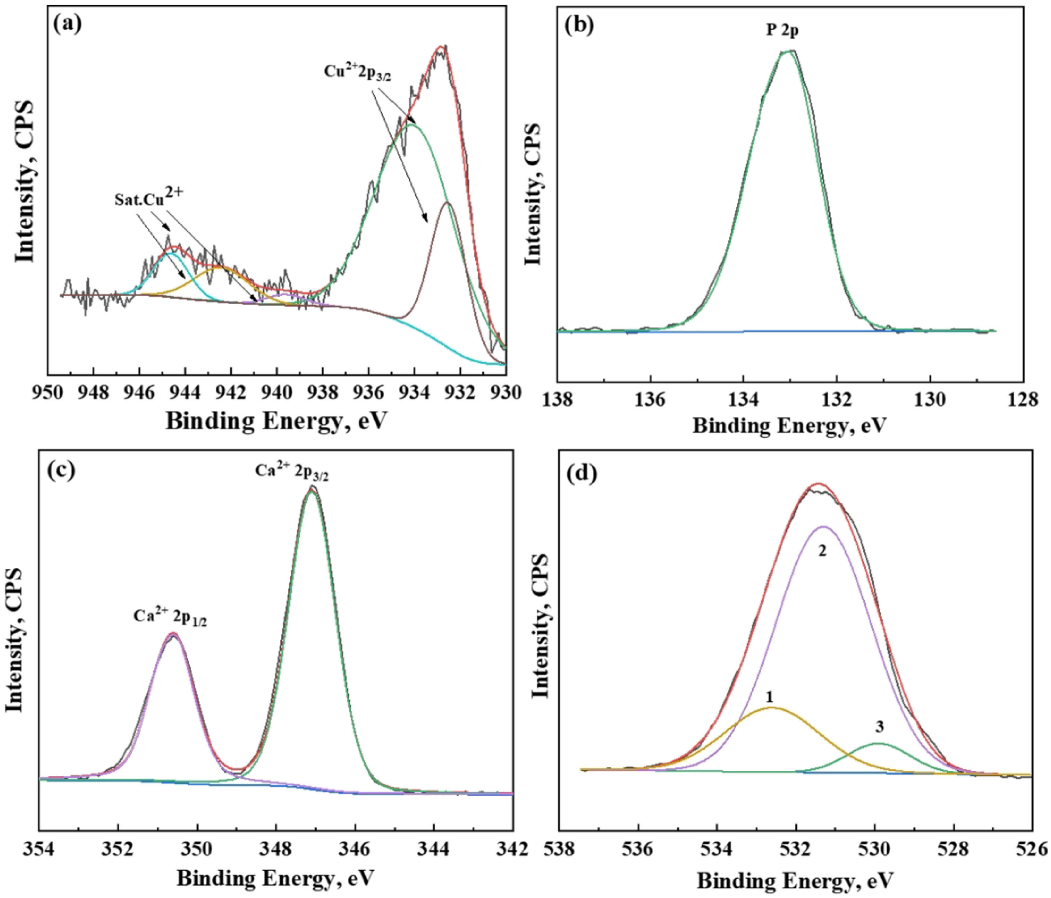

Fig. 3 XPS spectra of the CuHAp coating prepared in the electrolyte with Cu^{2+} concentration of 1.05 mmol/L: (a) Cu $2p_{3/2}$, (b) P 2p, (c) Ca 2p, (d) O 1s. Characteristic peaks: 1-O^{2-}; 2-PO_4, CO_3 and OH; 3-H_2O.

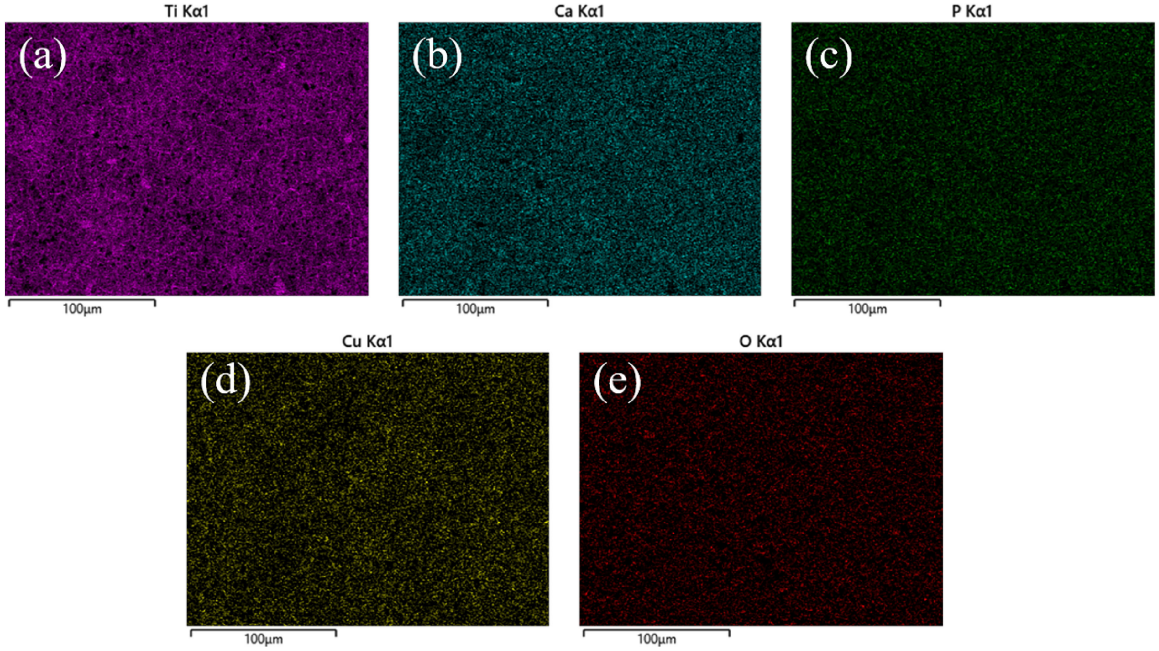

Fig. 4 Surface element distributions of the CuHAp coating prepared in the electrolyte with Cu^{2+} concentration of 1.05 mmol/L: (a) Ti, (b) Ca, (c) P, (d) Cu, and (e) O maps.

Cu^{2+} in the electrolyte was 1.05 mmol/L. Ti, Ca, P, Cu, and O were evenly distributed on the structural surface, and no elemental aggregation was observed.

Table 5 shows the EDS results measured on the surfaces of the samples prepared in the electrolyte with the four Cu^{2+} concentrations. With increasing Cu^{2+} concentration in the

Table 5 Compositions of the samples prepared in the electrolyte with different Cu^{2+} concentrations.

Group	Cu^{2+} concentration in electrolyte / mmol/L	Main elements (mass.%)						(Cu+Ca)/P molar ratio
		Cu	Ca	P	Ti	O	Cl	
(a)	0.525	1.03	1.06	2.24	90.83	3.93	0.90	0.59
(b)	1.05	1.57	2.98	3.58	86.74	4.74	0.38	0.86
(c)	2.1	3.56	6.02	6.74	68.32	14.59	0.59	0.95
(d)	4.2	6.85	12.33	12.57	55.15	12.47	0.62	1.03

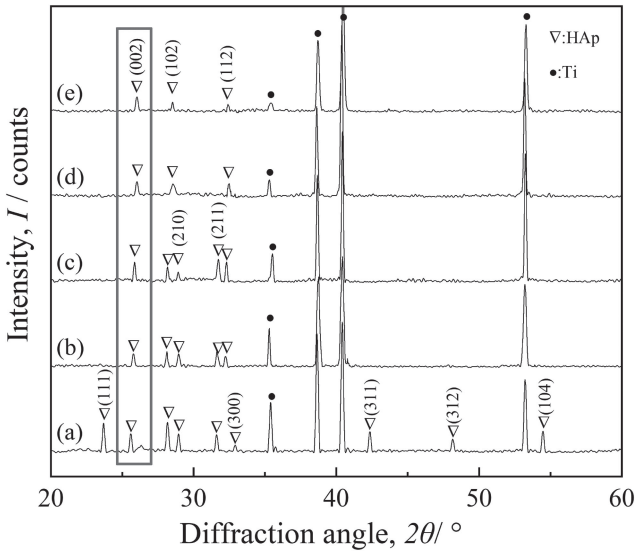

Fig. 5 XRD patterns of the HAp coating and CuHAp coatings prepared in the electrolyte with different Cu^{2+} concentrations: (a) HAp, (b) 0.525 mmol/L, (c) 1.05 mmol/L, (d) 2.1 mmol/L, and (e) 4.2 mmol/L.

electrolyte, the Cu content and (Cu + Ca)/P ratio increased, but the Ti content decreased, suggesting that the coating became thicker on the Ti substrate. By removing the Ti content, the percentages of Cu content in the coatings were calculated as 11.23%, 11.84%, 11.24%, and 15.27% in Groups (a)–(d), respectively.

Figure 5 shows the XRD patterns of the HAp coating and the CuHAp coatings prepared in the electrolyte with different Cu^{2+} concentrations. In addition to Ti, only peaks corresponding to HAp were observed in the patterns. The (002) diffraction peaks of all the CuHAp coatings shifted to higher angles compared with those of the HAp coating. It is known that the ionic radius of Cu^{2+} (72 pm)[31] is smaller than that of Ca^{2+} (99 pm).[32] The substitution of Ca^{2+} by Cu^{2+} in HAp resulted in a decrease in the lattice constant and caused the diffraction peaks to shift to higher angles.[33] The shift of the XRD peaks indicates that Cu was successfully doped into the coating.[34] The apatite crystallinity decreased with increasing Cu content, and some amorphous calcium phosphate (ACP) may have formed.

Table 6 Antibacterial rates of HAp coating and CuHAp coatings with different Cu contents.

Group	Antibacterial rate, η / %	
	Escherichia coli	Staphylococcus aureus
HAp	22.5	16.2
(a)	81.9	76.7
(b)	83.7	79.5
(c)	95.8	94.2
(d)	99.8	99.8

3.3 Antibacterial properties

Table 6 shows the antibacterial rates of the HAp and CuHAp coatings in Groups (a)–(d) against *E. coli* and *S. aureus*. The HAp coating absorbs drugs and acts as a carrier for antibiotics to inhibit bacteria,[35] but its antibacterial rate is low. When Cu was added to the HAp, the antibacterial rates of the CuHAp coatings in Groups (a)–(d) against *E. coli* and *S. aureus* were all greater than 70%. Coatings with antibacterial ability are deposited on the implant surface and can effectively kill the bacteria around the implant and prevent infection between the implant and bone tissue, further reducing the possibility of inflammation.[36] When the Cu content was 1.03%, the antibacterial rate of the coating reached 80%. With increasing Cu content, the antibacterial rate also increased. When the Cu content exceeded 3.56%, the antibacterial rate was greater than 90%, thus exhibiting excellent antibacterial properties.

Compared with HAp, ACP shows higher resorbability. The incorporation of a small amount of ACP changed the antibacterial properties of the coating. When the Cu content was 1.03%, the antibacterial rate was 81.9%, which was lower than that of a Cu-doped calcium phosphate coating[37] but higher than that of the Cu-doped HAp coating prepared by Xivaraj *et al.* (antibacterial rate >75% at Cu content of 0.8%).[38] This means that Cu^{2+} in calcium phosphate is easier to dissolve than Cu^{2+} in HAp, and so the antibacterial activity is higher. The Cu ions released by CuHAp exhibited a strong bactericidal effect on these bacteria, and the antibacterial rate of *E. coli* was slightly higher than that of *S. aureus*, indicating that the CuHAp coating had stronger antibacterial ability against *E. coli*. Studies have shown that Cu^{2+} can destroy the cell wall of *E. coli*, enter the cell

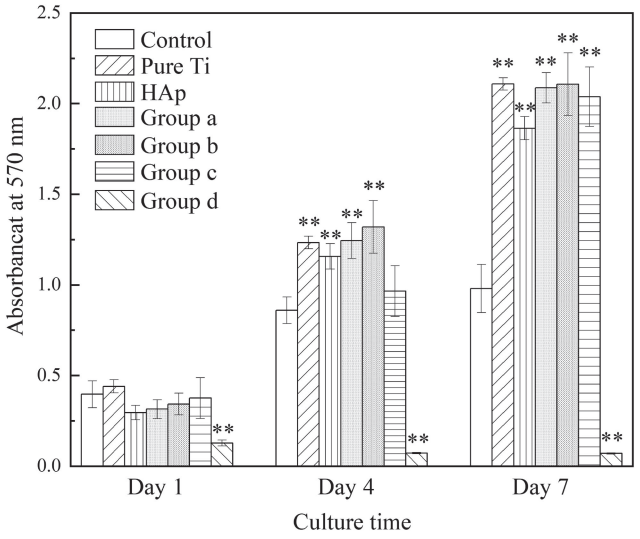

Fig. 6 Absorbance of MC3T3-E1 cells for each samples after 1, 4 and 7 days culture (**denotes a significant difference at $P < 0.01$ compared to control).

membrane, inhibit sugar transport and metabolism, destroy the balance of metal ions and enzyme systems, and kill *E. coli* altogether.[39)]

3.4 Cytocompatibility

Studies have shown that a Cu-containing surface can provide an antibacterial rate of ≥99.9%.[40)] However, the Cu content in a carbon-based coating required to achieve this high antibacterial activity is considerable, and a Cu content that is too high leads to cytotoxicity. Therefore, it is necessary to determine the Cu content required to balance the antibacterial activity and biocompatibility.

Studies have also shown that HAp coatings have excellent cell compatibility and bioactivity.[41,42)] According to Table 4, the Cu contents in Groups (a)–(d) were 1.03%, 1.57%, 3.56%, and 6.85%, respectively. Figure 6 shows the absorbance of MC3T3-E1 cells cultured on the surface of each coating for 1, 4, and 7 days. When the Cu content was 6.85%, the OD of the sample was low. In addition, with increasing culture time, the number of living cells did not increase significantly, indicating that cell vitality was very low. However, the difference was significant compared with the control group, pure Ti, the HAp coating, and the other CuHAp coatings ($P < 0.01$), after 1, 4, and 7 days of culturing. Other samples showed small differences in OD after 1 day of culturing, although the difference was not statistically significant. After 4 days of culturing, the OD values of the samples increased significantly, indicating that the number of cells in all samples proliferated with increasing culture time. Compared to the control, a statistically significant difference was found in pure Ti, HAp, and Groups (a) and (b). The OD values of the samples with low Cu contents of 1.03% and 1.57% [Groups (a) and (b)] were slightly higher than that of the HAp coating (not significant). At a Cu content of 3.56% [Group (c)], the OD of the coating was lower than that of the HAp coating with a statistically significant difference ($P < 0.05$). After 7 days of culturing, the number of cells in each sample further increased compared to that after 4 days. The OD values of pure Ti, HAp, and Groups (a), (b), and (c) were all significantly higher than that of the control ($P < 0.01$). No statistically significant difference was observed in the OD values between the CuHAp coatings [Groups (a), (b), and (c)] and the HAp coating. The results indicated that the CuHAp coatings containing trace amounts of Cu (1.03% and 1.57%) still exhibited good cell compatibility. Although the 3.56% Cu in the CuHAp coating decreased the cell vitality compared with the HAp coating after 4 days of culturing, the OD value was not lower than that of the control. Additionally, the OD value of Group (c) was significantly higher than that of the control but not lower than that of the HAp coating after 7 days of culturing. This suggests that the CuHAp coating containing 3.56% Cu also had good cytocompatibility. Studies have shown that HAp containing Cu releases a small amount of Cu into the implant, which is beneficial for maintaining cell proliferation.[43)] The release of Cu or the presence of Cu in the CuHAp coating promotes cell growth. Our experiment also showed that the release of Cu may promote cell survival and that the presence of Cu may change the surface potential to enhance cell adhesion.

4. Conclusion

In this study, a layer of copper-containing hydroxyapatite was successfully deposited on the surface of pure Ti via electrochemical deposition to obtain a CuHAp coating. The Cu content in the coating was controlled by changing the factors that had the greatest effect on the Cu content under the deposition conditions, and the effects of the Cu content on the surface morphology, antibacterial properties, and biocompatibility of the CuHAp coating were examined. The concentration of Cu^{2+} in the electrolyte had the greatest influence on the Cu content of the coating. When the Cu^{2+} concentration was 1.05 mmol/L (corresponding to a Cu content of the sample of 1.57%), the surface morphology of the coating was dense, uniform, and honeycombed. The antibacterial ability of the coating was significantly affected by the Cu content. The antibacterial rate of the CuHAp coating with low Cu content against *E. coli* and *S. aureus* were all greater than 70%. The antibacterial ability of the coating improved with increasing Cu content. When the Cu contents in the sample were 1.03% and 1.57%, good biocompatibility was achieved. When the Cu content was increased to 6.85%, cytotoxicity and low cell viability were observed. Therefore, the CuHAp coating with a Cu content of 1.57% had good surface morphology, antibacterial properties, and biocompatibility, and thus it would be a good candidate material for use in biomedical applications.

Acknowledgements

This work was partially supported by the Natural Science Foundation of Shanghai, China (No. 15ZR1428400), Shanghai Engineering Research Center of High-Performance Medical Device Materials (No. 20DZ2255500), and Grant-in-Aid for Scientific Research (C) (No. 20K05139) from the Japan Society for the Promotion of Science (JSPS), Tokyo, Japan.

REFERENCES

1) M. Niinomi: Mater. Sci. Eng. A **243** (1998) 231–236.
2) J. Lu, Y. Zhang, W. Huo, W. Zhang, Y. Zhao and Y. Zhang: Appl. Surf. Sci. **434** (2018) 63–72.
3) F. Li, X. Jiang, Z. Shao, D. Zhu and Z. Luo: Materials **11** (2018) 1391.
4) S. Spriano, S. Yamaguchi, F. Baino and S. Ferraris: Acta Biomater. **79** (2018) 1–22.
5) M. Stevanovic, M. Djosic, A. Jankovic, V. Kojic, M. Vukasinovic-Sekulic, J. Stojanovic, J. Oclovic, M.C. Sakac, R.K. Yop and V. Miskovic-Stankovic: J. Biomed. Mater. Res., Part A **108** (2020) 2175–2189.
6) A.A. Francis, S.A. Abdel-Gawad and M.A. Shoeib: J. Coat. Technol. Res. **18** (2021) 971–988.
7) A. Ritwik, K.K. Saju, A. Vengellur and P.P. Saipriya: J. Coat. Technol. Res. **19** (2022) 597–605.
8) S. Jose, M. Senthilkumar, K. Elayaraja, M. Haris, A. George, A.D. Raj, S.J. Sundaram, A.K.H. Bashir, M. Maaza and K. Kaviyarasu: Surf. Interfaces **25** (2021) 101185.
9) N.S. Jouda and A. Fadhel Essa: Mater. Today: Proc. (2021) 2214-7853.
10) S. Pang, Y. He, P. He, X. Luo, Z. Guo and H. Li: Colloids Surf. B **171** (2018) 40–48.
11) J.D. Avila, K. Stenberg, S. Bose and A. Bandyopadhyay: Acta Biomater. **123** (2021) 379–392.
12) D. Gopi, S. Ramya, D. Rajeswari, P. Karthikeyan and L. Kavitha: Colloids Surf. A **451** (2014) 172–180.
13) A. Anwar, S. Akbar, A. Sadiqa and M. Kazmi: Inorg. Chim. Acta **453** (2016) 16–22.
14) I. Uysal, F. Severcan, A. Tezcaner and Z. Evis: Prog. Nat. Sci.: Mater. Int. **24** (2014) 340–349.
15) H. Yang, B.J. Xiao and K.W. Xu: J. Mater. Sci.: Mater. Med. **20** (2009) 785–792.
16) M. Yazici, A.E. Gulec, M. Gurbuz, Y. Gencer and M. Tarakci: Thin Solid Films **644** (2017) 92–98.
17) B. Hu, N. Yin, R. Yang, S. Liang, S. Liang and F. Faiola: Sci. Total Environ. **725** (2020) 138433.
18) Ž. Radovanović, B. Jokić, D. Veljović, S. Dimitrijević, V. Kojić, R. Petrović and D. Janaćković: Appl. Surf. Sci. **307** (2014) 513–519.
19) M.M. Erol, V. Mouriño, P. Newby, X. Chatzistavrou, J.A. Roether, L. Hupa and A.R. Boccaccini: Acta Biomater. **8** (2012) 792–801.
20) R. Hang, A. Gao, X. Huang, X. Wang, X. Zhang, L. Qin and B. Tang: J. Biomed. Mater. Res., Part A **102** (2014) 1850–1858.
21) V. Stranak, H. Wulff, H. Rebl, C. Zietz, K. Arndt, R. Bogdanowicz, B. Nebe, R. Bader, A. Podbielski, Z. Hubicka and R. Hippler: Mater. Sci. Eng. C **31** (2011) 1512–1519.
22) H. Wu, X. Zhang, Z. Geng, Y. Yin, R. Hang, X. Huang, X. Yao and B. Tang: Appl. Surf. Sci. **308** (2014) 43–49.
23) N.-b. Li, W.-h. Xu, J.-h. Zhao, G.-y. Xiao and Y.-p. Lu: Thin Solid Films **646** (2018) 163–172.
24) K. Lee, Y.-H. Jeong, Y.-M. Ko, H.-C. Choe and W.A. Brantley: Thin Solid Films **549** (2013) 154–158.
25) S. Shanmugam and B. Gopal: Appl. Surf. Sci. **303** (2014) 277–281.
26) Y. Wang, S. Zhao, G. Li, S. Zhang, R. Zhao, A. Dong and R. Zhang: Mater. Chem. Phys. **241** (2020) 122360.
27) B.-O. Taranu, A.I. Bucur and I. Sebarchievici: J. Coat. Technol. Res. **17** (2020) 1075–1082.
28) M.C. Biesinger: Surf. Interface Anal. **49** (2017) 1325–1334.
29) T. Hanawa and M. Ota: Biomaterials **12** (1991) 767–774.
30) C. Battistoni, M.P. Casaletto, G.M. Ingo, S. Kaciulis, G. Mattogno and L. Pandolf: Surf. Interface Anal. **29** (2000) 773–781.
31) J. Luo, B. Mamat, Z. Yue, N. Zhang, X. Xu, Y. Li, Z. Su, C. Ma, F. Zang and Y. Wang: Colloid Interface Sci. Commun. **43** (2021) 100435.
32) U. Batra, S. Kapoor and S. Sharma: J. Mater. Eng. Perform. **22** (2013) 1798–1806.
33) V. Stanić, S. Dimitrijević, J. Antić-Stanković, M. Mitrić, B. Jokić, I.B. Plećaš and S. Raičević: Appl. Surf. Sci. **256** (2010) 6083–6089.
34) W. Hu, J. Ma, J. Wang and S. Zhang: Mater. Sci. Eng. C **32** (2012) 2404–2410.
35) J. Jiang, G. Han, X. Zheng, G. Chen and P. Zhu: Surf. Coatings Technol. **375** (2019) 645–651.
36) S. Shanmugam and B. Gopal: Ceram. Int. **40** (2014) 15655–15662.
37) Q. Li, J. Yang, J. Li, R. Zhang, M. Nakai, M. Niinomi and T. Nakano: Mater. Trans. **62** (2021) 1052–1055.
38) Y. Huang, X. Zhang, R. Zhao, H. Mao, Y. Yan and X. Pang: J. Mater. Sci. **50** (2015) 1688–1700.
39) D. Sivaraj, K. Vijayalakshmi, A. Ganeshkumar and R. Rajaram: Int. J. Pharm. **590** (2020) 119946.
40) Y.-H. Chan, C.-F. Huang, K.-L. Ou and P.-W. Peng: Surf. Coat. Technol. **206** (2011) 1037–1040.
41) Y.-J. Guo, T. Long, W. Chen, C.-Q. Ning, Z.-A. Zhu and Y.-P. Guo: Mater. Sci. Eng. C **33** (2013) 3583–3591.
42) D.O. Costa, P.D.H. Prowse, T. Chrones, S.M. Sims, D.W. Hamilton, A.S. Rizkalla and S.J. Dixon: Biomaterials **34** (2013) 7215–7226.
43) S. Gomes, C. Vichery, S. Descamps, H. Martinez, A. Kaur, A. Jacobs, J.-M. Nedelec and G. Renaudin: Acta Biomater. **65** (2018) 462–474.